

# In Vitro Development of an Acellular Biological Liver Scaffold Repopulated with Rat Hepatocytes

Tanya Debnath<sup>1</sup>, Kancherla Ravindranath<sup>2</sup>, Chandra Shekar Mallarpu<sup>3</sup>, Pavan Mujawdiya<sup>4</sup>, Suman Kapur<sup>4</sup> and Lakshmi Kiran Chelluri<sup>3\*</sup>

<sup>1</sup>Global Medical Education and Research Foundation, Hyderabad, Telangana, India

<sup>2</sup>Institute of Gastroenterology, Gleneagles Global Hospitals, Hyderabad, Telangana, India

<sup>3</sup>Transplant Immunology and Stem Cell Unit, Gleneagles Global Hospitals, Hyderabad, Telangana, India

<sup>4</sup>Department of Biological Sciences, Birla Institute of Technology and Science – Pilani, Hyderabad Campus, Hyderabad, Telangana, India

## Abstract

The increasing demand of organs for transplantation necessitates the development of substitutes to meet the structural and physiological functions. Tissue decellularization and recellularization aids in retaining the three-dimensional integrity, biochemical composition, tissue ultra-structure, and mechanical behavior, which makes them functionally suitable for organ transplantation. Herein, we attempted to rebuild functional liver grafts in small animal model (Wistar rat) with a potential of translation. A soft approach was adopted using 0.1% SDS (Sodium Dodecyl Sulfate) for decellularization and primary hepatocytes were used as potential cell source for recellularization. The decellularization process was evaluated and confirmed using histology, DNA content, ultra-structure analysis. The resultant scaffold was re-seeded with the rat hepatocytes and their biocompatibility was assessed by its metabolic functions and gene expression. The structural components of the ECM (Laminins, Collagen type I, Reticulins) were conserved and the liver cell specific proteins like CK18, alpha fetoprotein, albumin were expressed in the recellularized scaffold. The functionality and metabolic activity of the repopulated scaffold was evident from the albumin and urea production. Expression of Cytokeratin-19 (CK-19), Glucose 6- Phosphatase (G6P), Albumin, Gamma Glutamyl Transferase (GGT) genes has distinctly confirmed the translational signals after the repopulation process. Our study clearly elucidates that the native extracellular matrix of rat liver can be utilized as scaffold for effective recellularization for whole organ regeneration.

**Keywords:** Decellularization; Recellularization; Extracellular matrix; Liver; Tissue regeneration

## Introduction

Solid organ regeneration is an emerging area in tissue engineering, providing tissue constructs with functional remodeling, and potential to re-integrate into host systems [1]. Recent tissue engineering approaches provide biological scaffolds composed of extracellular matrix (ECM) controlling cell functions and promoting new tissue formation. Biomaterials were employed as scaffolds for the incorporation of required cell types which intrinsically modulate the tissue microenvironment. Various natural biopolymers have been used as scaffolds to mimic the extra cellular matrix of the tissues *in vitro*. These biopolymer-based scaffolds and the three-dimensional (3D) culture systems conserve the cell phenotype and supports their proliferation [2,3]. The biological signaling for cell adhesion and proliferation is constantly regulated by the scaffold proteins which are being modulated based on the metabolic and functional requirements of the healthy tissues and organs [4]. Intact three-dimensional extracellular matrices from different allogeneic and xenogeneic tissue sources are known to preserve the cellular phenotypes with the help of obligatory ligands and bioactive molecules during the process of tissue regeneration [5,6]. Further, the natural ECM of the tissues is advantageous over conventional two-dimensional and three-dimensional culture systems, as they maintain and retain the complex microstructure and functional proteins [7].

The current focus is on the use of native biological scaffolds as transplantable organ which can be employed for clinical use. In this context, numerous techniques for decellularization have been developed for various tissues/organs. This helps to remove cellular and nuclear content, along with the immunogenic antigens, while preserving the ECM architecture and structural components, such as collagen, elastin networks along with the biochemical constituents [8].

There are a variety of approaches such as chemical, enzymatic and physical methods for effective decellularization of whole organs

[9]. However, other bioactive ligands such as integrins, cadherins, are also important for cell-cell interaction, cell-ECM interaction, and new ECM formation [10]. The tissue ultra-structure, matrix density and architecture vary among different types of organs and hence play a major role in utilization of decellularization techniques. In case of a complex and dense organ such as liver, decellularization is usually achieved through use of the hepatic vascular network and dynamic culture systems which can support the delicate vasculature of the organ during processing [11]. Completely decellularized organs or tissues can eradicate antagonistic immune response elicited by cell membrane epitopes, allogeneic or xenogeneic DNA, and damage-associated molecular pattern molecules [12].

The process of decellularization and recellularization for tissues and organs regeneration has emerged as remarkably promising approach and several attempts are made to mimic the *in vivo* conditions, using perfusion techniques [13]. The progression of organ development technology involves appropriate tissue niche or microenvironment and well-integrated and vascularised extracellular matrices. The recellularization of the native ECM can be done by various cells types like stem cells, iPSCs etc. However, freshly isolated primary hepatocytes (epithelial cells) were utilised to investigate the various aspects of liver recellularization and metabolism [14].

**\*Corresponding author:** Lakshmi Kiran Chelluri, Transplant Immunology and Stem Cell Unit, Gleneagles Global Hospitals, Lakdi-ka-Pool, Hyderabad, Telangana, India, Tel: 04030244501; E-mail: [lkiran@globalhospitalsindia.com](mailto:lkiran@globalhospitalsindia.com)

**Received** April 11, 2019; **Accepted** April 19, 2019; **Published** May 01, 2019

**Citation:** Debnath T, Ravindranath K, Mallarpu CS, Mujawdiya P, Kapur S, et al. (2019) *In Vitro* Development of an Acellular Biological Liver Scaffold Repopulated with Rat Hepatocytes. J Tissue Sci Eng 10: 224.

**Copyright:** © 2019 Debnath T, et al. This is an open-access article distributed under the terms of the Creative Commons Attribution License, which permits unrestricted use, distribution, and reproduction in any medium, provided the original author and source are credited.

The hepatocytes of the liver comprise 80% of all the liver cells and they have a fundamental role in liver function. The recellularization strategies are being improved by finding clinically relevant cell type from a renewable tissue source and a competent cell seeding methods [15,16]. Thus, we optimised *in vitro* methods to reconstitute the acellular liver scaffold, with cell populations that distinctively re-integrate within the biomimetic ECM to generate functional hepatic tissue with a potential treatment approach for chronic liver diseases.

The density of the liver along with the fragility of the hepatic ECM necessitates the use of mild detergents for quick decellularization for effective cell removal. We tried to optimize and simplify the technique of decellularization in order to make it more economical for with minimal damage to the liver ECM. The native biological liver scaffold facilitates cues for the migration, adhesion and differentiation of liver epithelial cells for their development and hepatic functioning governed by cell-ECM interactions. Thus, we utilised portal vein (PV) as cell seeding route and primary rat hepatocytes as a cell source for recellularization. We also assessed the stability, integrity of ECM components and metabolic functionalities of the recellularized liver grafts.

## Materials and Methods

SDS and Triton X-100 were purchased from Sigma-Aldrich, St. Louis, MO, USA. The required concentrations of SDS and Triton X-100 were made in autoclaved distilled water. Collagenase and dispase were procured from Gibco, Life technologies, USA. The required antibodies were procured from Abcam (Cambridge, United Kingdom) and Novus Biologicals (Colorado, United States).

## Animals

All animal procedures were conducted with prior approval from Jeeva Life Sciences Pvt. Ltd, Hyderabad institutional animal ethical committee (IAEC) ref no. CPCSEA/IAEC/ JLS/006/01/17/004 and all the protocols were followed as per the approved guidelines. Adult Wistar rats weighing 100-150 g were used for the development of decellularized liver scaffolds. Pathogen free rats were maintained under controlled environmental conditions with free access to food and water.

## Rat liver decellularization by detergent based perfusion method

Wistar rats (n=5) were anesthetized based on IACUC (Institutional Animal Care and Use Committee) guidelines for anesthesia using ketamine (100 mg/kg) and xylazine (10 mg/kg) per body weight using intra-peritoneal route, followed by topical skin disinfection. All the animals received necessary care based on criteria by Guide for the care and use of laboratory animals. A transverse incision was made in the abdomen, which exposed the portal vein, the bile duct, and the inferior vena cava. The portal vein was successfully cannulated with a 24-gauge (BD, Biosciences, USA) needle and connected to the infusion pump (Infusomat®P B Braun). The liver was initially perfused with 1X PBS for an hour then continuously perfused with 0.1% SDS in distilled water for 3 hr at a flow rate of 5 mL/min. Subsequently, liver was washed with distilled water for 15 min, followed with 0.1% Triton X-100 for 30 min to remove other bound nucleic acids. The completely decellularized liver was washed extensively and preserved in PBS containing penicillin (100 IU/mL), streptomycin (100 IU/mL), gentamycin (50 IU/mL), amphotericin B (2.5 µg/mL), at 4°C until further use.

## Quantification of DNA and collagen of decellularized liver matrix

Decellularized liver matrices and fresh rat liver tissues were used

for quantification of total DNA. Briefly, total DNA was isolated from equal volumes of decellularized and fresh liver tissues using a commercially available kit (DNeasy Blood and Tissue Kit, QIAGEN). The DNA concentration was estimated at 260 nm using a NanoDrop spectrophotometer (ND-2000c; Thermo, USA) (n=5).

The collagen content in the native tissue and decellularized tissue was quantified using Sirius red colorimetric assay. Briefly, tissues were homogenised using a tissue homogeniser and the homogenate was centrifuged at 12,000 Xg for 30 min at 4°C. The pellet was dried using vacuum concentrator and dissolved in 1X PBS and plated for further estimation. The collagen standards ranging from 15-90 µg were made as serial dilution in PBS and added to each well in triplicates. 65 µg Sirius red stain (Direct Red 80, Sigma) in saturated picric acid was added and incubated for 30 min at 37°C on a rocker. The plates were spun at 10,000 Xg for 30 min at 4°C. The pellet was dissolved in 0.1 N NaOH for 30 min and read on a spectrophotometer at 530 nm absorbance (n=5).

## Isolation of primary rat hepatocytes

Primary adult hepatocytes were isolated from Wistar rats weighing 100-150 gm, using a modified collagenase and dispase perfusion technique. Rats were anesthetized using ketamine (100 mg/kg) and xylazine (10 mg/kg) per body weight intra-peritoneally, followed by cannulation. The liver was initially perfused with 1X PBS solution, followed by the perfusion with pre-warmed collagenase type IV (0.05%) and dispase (0.3%) combined solution at rate of 300 ml/hr. After the liver turns mushy it was excised and minced gently in cold William's E media (Gibco, USA). The suspension was filtered through 70 µm cell strainer (BD Biosciences, USA) and centrifuged at 50 Xg for 5 min. The cell pellet was re-suspended in complete William's E media and viability was assessed using trypan blue.

## Reseeding of the decellularized liver scaffold

The decellularized liver matrix was washed with PBS and antibiotics and perfused using complete William's E media supplemented with 10% FBS and 0.0036 µg/mL insulin (sigma, USA), 10 ng/mL epidermal growth factor (Sigma-aldrich, USA), penicillin (100 IU/mL), streptomycin (100 IU/mL), gentamycin (50 IU/mL) through the portal vein prior to recellularization. A total of 60 million cells were resuspended in 20 mL of culture medium and perfused into the scaffold slowly at a flow rate of 1 mL/min using an infusion pump (Infusomat®P B Braun). The injected cells were retained in the liver scaffold as a static culture and then complete media was perfused into the scaffold continuously using the perfusion pump at a flow rate of 0.5 mL/min. The entire perfusion system was placed in 5% CO<sub>2</sub> incubator at 37°C. The perfusate was collected and replaced with the fresh media for 14 days.

## Characterization of the decellularized and recellularized liver matrix

**Histological staining:** Normal fresh liver, decellularized liver matrix and recellularized liver scaffolds were fixed in 10% neutral buffered formalin at room temperature for 24 h (n=5). The paraffin fixed tissue samples were sectioned into 5 µm sections followed by staining with Hematoxylin and eosin (H&E) and Masson's trichrome (MT) as per standard staining protocols.

**SEM analysis:** Scanning electron microscopy (SEM) was used to observe the microstructure of the ECM in the decellularized liver and recellularized as well as the fresh rat livers (n=5). Samples were fixed in Karnovsky's fixative (pH 7.2) for 24 h at 4°C. Following washing with 0.1 M phosphate buffer, samples were dehydrated in a graded ethanol-water

series upto 100% ethanol. Specimens were dried at critical point using CO<sub>2</sub> and images were recorded with a scanning electron microscope (S-3400N, HITACHI).

**Immunostaining:** The ECM components in the decellularized matrix were determined by fluorescent staining for the presence of collagen type I, laminin and reticulins. Recellularized scaffolds were characterised for the presence of hepatocyte specific proteins like CK-18, Alpha fetoprotein (AFP), Glucose 6 phosphate dehydrogenase (G6PD) and Albumin. Briefly, the liver scaffolds were fixed in 4% formaldehyde solution and embedded in paraffin. The paraffin blocks were sectioned at 5 µm thickness. Slides were rehydrated, washed with 1X PBS and blocked using Bovine Serum Albumin (BSA) for 30 min at 37°C. Decellularized tissue sections and sections from fresh rat liver tissues were incubated with primary antibodies such as collagen type I (dilution 1:200), laminin (dilution 1:200), and reticulins (dilution 1:100) overnight at 4°C.

Recellularized scaffold sections were incubated with primary antibodies G6PD (2 µg/mL concentration), albumin (dilution 1:500), AFP (20 µg/mL concentration). After washing in PBS, slides were incubated with secondary goat anti rabbit Alexa 568 and Alexa 488 for 1 hr at 37°C. Cytokeratin-18 antibody (CK-18) (dilution 1:200) was already tagged with Alexa 488 fluorochrome and thus, recellularized liver sections were incubated for 1 hour at 37°C. Later, all the tissue sections were mounted using mounting medium (Vectashield containing DAPI (4', 6'-diamidino-2-phenylindole dihydrochloride) (Abcam, Cambridge, UK) and incubated for 2-3 min at 37°C in dark. The imaging was performed using a confocal laser microscope (Leica TCS, CLSM) and the images were processed using Leica software (n=5).

### Assessment of recellularized liver function

The culture medium of the continuously perfused recellularized liver graft was collected periodically. Albumin and urea content in the culture media were measured using the Agilent bioanalyzer (Agilent Technologies, USA) according to the manufacturer's instructions.

### Quantitative reverse transcription PCR

Total RNA was extracted using a TRIZOL method and 100-200 ng of total RNA was reverse transcribed into cDNA using ProtoScript First strand cDNA conversion kit (New England Biolabs, France) as per manufacturers' instructions. Primers for the amplification of albumin, G6P, CK19, GGT, and actin-beta (ActB) were generated as shown in Table 1. Quantitative RT-PCR assay was performed using SYBR-green PCR Master Mix (Applied Biosystems, USA) on the StepOne™ Real Time PCR system. Each experiment was performed in triplicate, and the gene expression levels were normalized to the levels of ActB.

### Statistical analysis

All data were analyzed using SPSS statistical software and using Student's t-test. All values and graphs represented as mean ± standard deviation (SD). The error bars represent the standard error of the mean. Statistical significance was defined as p<0.05.

## Results

### Decellularized liver scaffolds

The cannulated liver gradually turned light brown color to white and translucent with the removal of cellular material upon perfusion with 0.1% SDS, an anionic detergent that lyses cells and solubilises cytoplasmic components and membrane lipid. 0.1% Triton X-100, a non-ionic surfactant for the recovery of membrane components under mild non-denaturing conditions assisted the removal of bound nucleic acids as manifested from the visible vasculature of slender veins. The microvascular networks and blood vessels were preserved in the decellularized matrix as evident from Figure 1a.

The H&E staining of the resultant liver scaffold showed no residual cells. Whereas, the Masson's trichrome staining showed the presence of collagen fibre maintained as tubular structures in the liver ECM. However, no cellular staining was seen in the liver matrix. The normal fresh rat liver was used as the control and the cellular components was stained by H&E and MT staining along with the blue colour stained conserved collagen matrix. The decellularization was also confirmed by SEM where no cells were observed within the decellularized liver matrix. The extracellular matrix showed networks of collagen fibers with lamellar structures with intact large and small vessels. The matrix had arrangements of connective tissue fibers clearly defining parenchymal free spaces. The rat liver samples without treatment retained their extracellular matrix with fibers arranged in honey-comb like pattern with proper distribution of the cellular components and hepatocytes (Figure 1b).

### Evaluation of ECM protein components of decellularized liver

These matrix proteins were preserved as indicated by structural and basement membrane components of the ECM in the decellularized liver scaffolds. More specifically, laminin was predominantly found in the basement membrane of larger blood vessels and the liver matrix whereas, collagen type I was preserved in the sinusoids and the portal ducts. The reticulin staining demonstrated the presence of reticular fibers in the parenchymal matrix of the decellularized tissues without any nuclear component (no DAPI staining). The native fresh rat liver also demonstrated similar expression of extracellular matrix proteins along with the preserved nucleus as shown by DAPI staining (Figure 2a-2h).

### DNA and ECM collagen content

The residual DNA content was significantly decreased in the decellularized matrix as compared to normal untreated rat liver tissues, 11 ± 4 µg/mL and 980 ± 18 µg/mL respectively. DNA quantification also confirmed the decellularization process indicating the absence of the nuclear material in the scaffold as compared to the fresh liver tissue (Figure 2i).

The collagen content was estimated in the liver matrix after decellularization. The standards were fit to a 4-parameter curve,

Gene	Forward primer	Reverse primer
Alb	CGAGAAGCTTGGAGAATATGG	GTCAGAGCAGAGAAGCATGG
G6P	TGCATTCTGTATGGTAGTGG	GAATGAGAGCTCTTGGCTGG
CK19	GTGCCACCATTGACAACTCC	AATCCACCTCCCACTGACC
GGT	ATGAGCTCTGAGTTCTAGGCC	CCACAGCTCTTTCACATCG
ActB	TGGAGAAGAGCTATGAGCTGC	GATCCACATCTGCTGGAAGG

**Table 1:** List of primers. Abbreviations: Alb, albumin; G6P, glucose 6-phosphatase; CK19, cytokeratin, GGT, gamma-glutamyl transpeptidase; ActB, actin-beta.

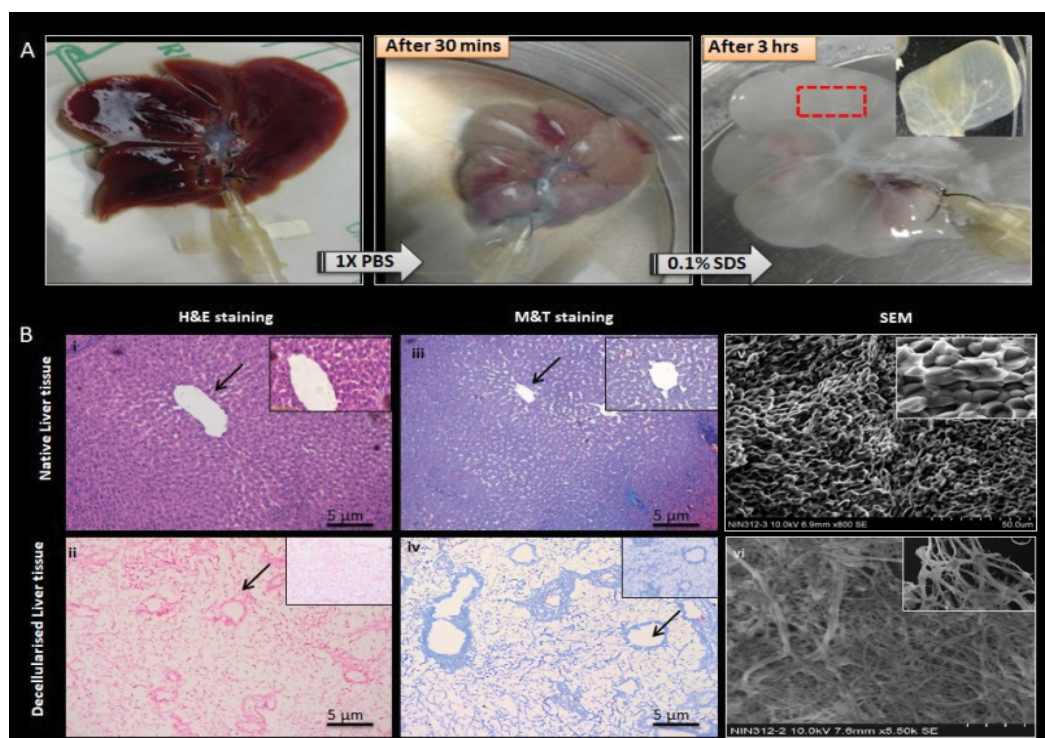


**Figure 1:** Decellularized whole rat liver. a) Schematic representation of the decellularization process the native rat liver turns light brown after 1X PBS perfusion and gradually turns white and then translucent with 0.1% SDS after 4 hrs. The complete decellularization was evident from the appearance of visible vascular networks and clear veins. b) Hematoxylin and Eosin staining of native rat liver and decellularized rat liver showing presence and absence of nucleic material (blue), respectively. Masson's trichrome staining of native rat liver showing presence of collagen (blue), pink cytoplasm while the decellularized rat liver shows the presence of abundant collagen but absence of cytoplasm and nuclei respectively. The arrows indicating the presence of blood vessels. SEM images of native rat liver tissue shows the presence of populated hepatocytes throughout the liver matrix. Decellularized rat liver matrix without the cellular content along with networks of ECM fibers with lamellar structures was observed.

$R^2=0.99$ . However, collagen content in the decellularized matrix slightly decreased when compared to the native tissue i.e.,  $49 \pm 6 \mu\text{g}/\text{mg}$  wet tissue and  $53 \pm 7 \mu\text{g}/\text{mg}$  wet tissues respectively as shown in Figure 2j. This indicates that the enzymatic decellularization processes maintained the original native tissue structure and components to a major extent without altering the extracellular matrix component.

### Re-seeding liver matrix with adult hepatocytes

Primary rat hepatocytes were successfully isolated by one step collagenase and dispase perfusion method. An average yield of  $60\text{--}70 \times 10^6$  cells/mL was obtained and  $>85\%$  cell viability was confirmed by trypan blue. The adult freshly isolated hepatocytes were infused through the portal vein and the cells were aggregated in the liver graft gradually in order to prevent the shear stress and minimize the mechanical damage to engrafted cells. The decellularized liver scaffold was initially primed with culture medium aiding homogenous distribution and proliferation of the hepatocytes in the liver scaffold (Figure 3a).

The histological evaluation by H&E and MT staining revealed that majority of cells were distributed throughout the scaffold. Furthermore, engrafted cells were distributed around central veins, which indicated that hepatocytes entered the ECM near the portal area of the parenchyma and beyond. Subsequently these cells reached the peri-central area across the lobular honey-combed ECM as evident from the SEM analysis. SEM images of reseeded liver graft after 14 days of perfusion culture displayed that hepatocytes were engrafted around the vessels and repopulated the surrounding parenchymal area (Figure 3b).

Immuno-histochemical staining of recellularized liver sections confirmed the localization of the hepatocytes, throughout the liver ECM. The liver epithelial cells i.e., hepatocytes seeded through the PV were well engrafted within the liver scaffold which was well evident with the expression of liver-specific proteins like albumin, CK-18, GG6P and AFP along with the nucleus stained with DAPI (Figure 3c).

### Biocompatible recellularized 3D liver graft

The functionality and metabolic activity of the infused hepatic cells were analyzed by quantification of albumin and urea. The cumulative urea production increased remarkably after 5 days of culture i.e.,  $20 \pm 0.45 \text{ mg}/10^6$  cells and albumin synthesis improved to  $6 \pm 0.23 \mu\text{g}/10^6$  cells after 2 days as shown in Figure 4. This increase can be attributed to the proliferation of the hepatocytes within the liver matrix ( $n=5$ ).

### Gene expression of the recellularized liver

To characterize the kinetics of the changes in gene expression occurring as consequence of hepatocyte infusion in the decellularized liver scaffold, we performed quantitative RT-PCR of well-known liver specific genes namely, CK-19, GG6P, Albumin, GGT and Act B as house-keeping gene. Gene expression has distinctly confirmed the translational signals after the repopulation process. Expression of CK-19, GGT and G6P increased approximately 2-4-fold after 14 days of culture. Progressive increase of hepatocyte markers like albumin and CK 19 during the culture period indicated appropriate repopulation of decellularized liver graft as demonstrated in Figure 5. All the liver

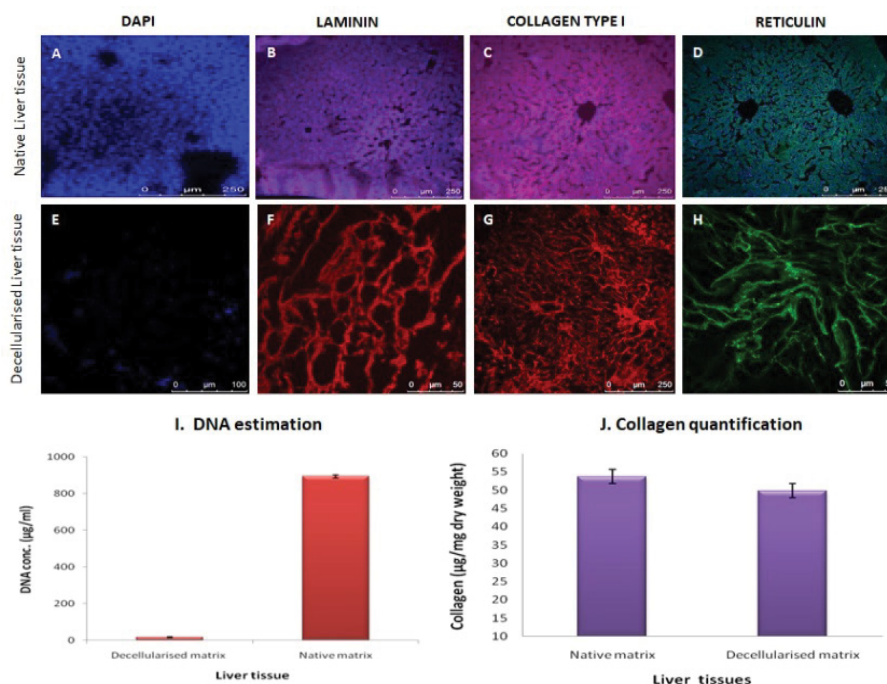


**Figure 2:** Determination of ECM and cellular components. Specific ECM proteins and the cellular components of the acellular liver bio-scaffold comparison with fresh rat liver tissue were studied. (A-D) Immunostaining results of the fresh liver showed collagen type I, laminins and reticulins mostly around larger vessels and also throughout the parenchymal spaces consistent with their localization of nuclear staining with DAPI. (E-H) similarly, the ECM proteins (Collagen type I and laminins) were observed around vascular basal membrane and parenchymal areas of the acellular liver bioscaffold. Reticulin staining demonstrated the presence of reticular fibers in the parenchymal matrix of the decellularized tissues. However, the nuclear component was not visible in the decellularized liver matrix upon staining with DAPI. (I) The residual DNA content decreased significantly in the decellularized rat livers ( $11 \pm 4 \mu\text{g/ml}$ ) as compared to normal rat livers ( $980 \pm 18 \mu\text{g/ml}$ ) measured per mg wet tissue weight. (J) Collagen content in the native liver tissue was  $53 \pm 7 \mu\text{g/mg}$  wet tissue whereas, the collagen content of the decellularized matrix decreased to  $49 \pm 6 \mu\text{g/mg}$  wet tissue yet indicating that the fibrillary collagen of the native liver was retained after decellularization process.

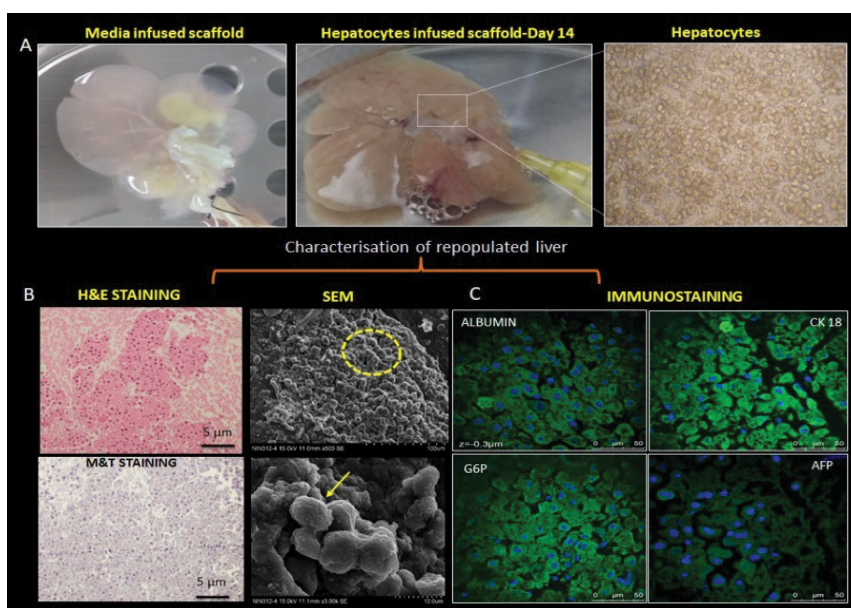


**Figure 3:** Re-population and characterization of rat liver scaffold. (A) The well-preserved liver scaffold was initially infused with the hepatocyte culture medium. Freshly isolated primary rat hepatocytes were infused into the scaffold through the PV of the decellularized liver. The decellularized liver was fully populated with hepatocytes and continuously perfused with the culture medium for the proliferation and functioning of the engrafted cells. (B) The H&E and MT staining of the reseeded liver graft showed uniform distribution of the hepatocytes throughout the liver section. The hepatocytes were repopulated around the vessels and the surrounding parenchymal spaces throughout ECM as evident from SEM analysis. The arrow indicating group of hepatocytes in the scaffold. (C) The liver specific proteins like albumin, CK 18, G6P and AFP expression was observed (green fluorescence) on the cell surfaces and the nucleus was stained with DAPI (blue) of repopulated liver section.

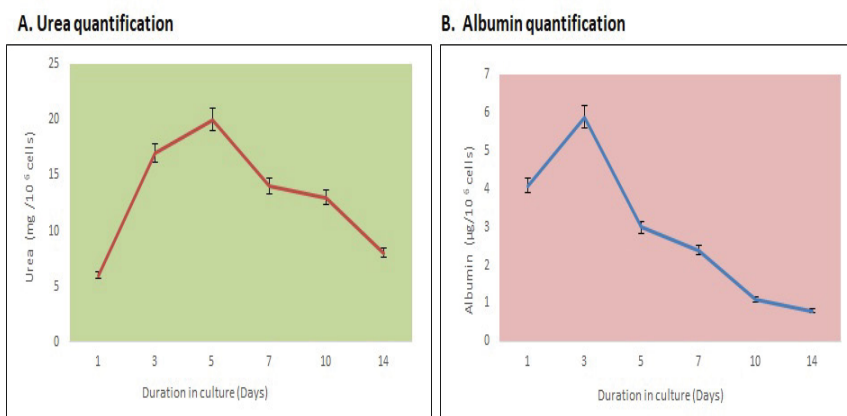


**Figure 4:** *In vitro* functional evaluation. (A) The urea synthesis by the recellularized liver graft increased continuously in the culture medium from day 3 to day 7. (B) The metabolism of the hepatocytes was well evident from the higher albumin production after 2 days (n=5).

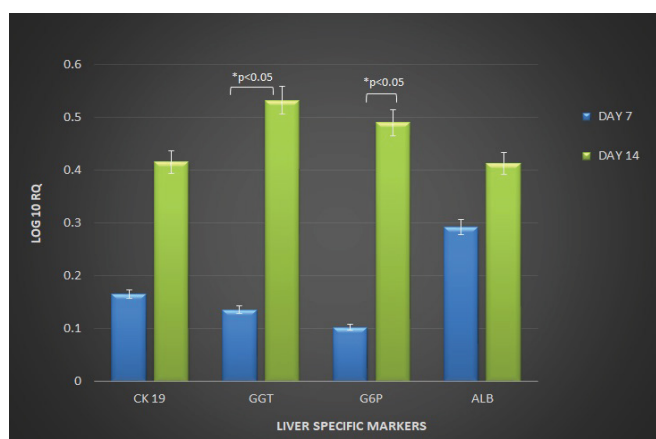


**Figure 5:** Expression of liver specific genes. The expression of liver specific genes of the recellularized liver graft was evaluated by qPCR analysis. The graph indicates the expression levels of various liver specific genes on different days. The data revealed increased levels of ALB, CK 19, GGT and G6P genes by day 10. However, GGT and G6P gene expression was significantly higher after 10 days culture as compared to the preliminary expression levels. Data is expressed as mean  $\pm$  SD with significance at  $p<0.05$ .

specific genes have shown an increase in their expression heading towards the development of a recellularized liver graft (n=5).

## Discussion

Whole organ decellularization techniques have emerged as a new therapeutic strategy for organ regeneration by generating natural tissue matrices. Earlier Uygun et al. reported whole liver regeneration using perfusion based decellularized of liver scaffolds and transplantation of recellularized liver grafts [17]. The tissue architecture and composition along with the ECM regulates the maintenance of cell phenotypes and differentiation in a specific tissue. Nevertheless, the composition of the ECM can get altered following various decellularization methods, which results in the amendment of cell proliferation and differentiation. Among the various decellularization processes being studied widely, continuous vascular perfusion is a technique that is intended to preserve the three-dimensional architecture of an organ while eliminating the parenchymal cell population [18]. Hence, we report the perfusion through the portal vein as an efficient method in the delivery of de-cellularising agents into the tissue owing to the close proximity of the vascular network. Mild concentration of SDS (0.1%) has been

standardized for continuous perfusion, considering the complex liver density with abundant cellular enzymes and delicate hepatic ECM. The decellularization process was aimed for a lesser duration with intent of maintaining the integrity and preserving the niche for subsequent recellularization process.

Our results confirm the study published by Pan et al. where the rat liver was decellularized using 0.1% SDS through the portal vein and hepatic artery [19]. SEM images also confirmed the complete decellularization of the liver tissue with compact three-dimensional architecture, lamellar structures and intact large and small vessels as reported by Xu et al. [20]. The ECM components, including collagens, are highly conserved between species, and do not cause obvious immune responses and these needs to be retained in the process of whole organ decellularization in order to prevent the collapse of the internal porous structure and flexible deformation [21,22]. The mild treatment with SDS preserved the collagen of the liver matrix which is important for maintenance of native physiological and structural tissue compliance. Thus, equilibrium was attained between the removal of the cellular components and the vascular integrity of the resulted 3D liver scaffold.

The experimental data reported preserved matrix components (laminin, collagen type I, reticulins) of the decellularized liver which are required for the maintenance of the tissue microenvironment. A previous study by Yeung et al. was found similar to our results on the effect of SDS on extracellular matrix components of tissues [23].

The preserved structural components of liver ECM can support remodeling of functional hepatic tissue with appropriate cell types. The hepatocytes are well known to perform most of the liver functions in conjugation with several other cell types for body metabolism and survival. Hepatocytes tend to lose their phenotype in 2D cultures but retain their characteristics in mechanically and chemically conserved 3D microenvironment [24]. Thus, we developed a convincing therapeutic approach towards the recellularization to achieve a functional 3D biological liver graft with appropriate tissue metabolism.

Further, we introduced adult hepatocytes through portal vein perfusion into acellular liver matrix to assess their successful migration and re-population within liver parenchyma. The perfusion via portal vein allows access to the hepatic vessels enabling improved repopulation of vasculature throughout the scaffold. Our study suggests that rat liver scaffold provided the appropriate spatial distribution of cells for homing and maturation in the presence of oxygen and nutrient gradients. The continuous medium perfusion provides large interaction of the proliferating hepatocytes with the extracellular matrix aiding in effective removal of metabolic waste [25]. The cells injected into the acellular rat liver scaffold expressed typical hepatic, endothelial and biliary epithelial markers found comparable to a study by Baptista et al. [26]. Also, a report by Navarro et al. showed that human liver stem cells can be also differentiated into matured hepatocytes in acellular scaffolds [27]. We also observed the presence of hepatocytes in the parenchymal spaces outside the microvasculature as reported by Uygun et al. which was attributed to loss of sinusoidal integrity in the absence of the liver sinusoidal endothelium and other non-parenchymal cells [28].

The decellularized liver matrix was infused with approximately 60 million cells and was seeded efficiently via portal vein this was earlier reported adequate to restore liver function in animal models by Fox et al. [29]. The retained ECM constituents like collagen, fibronectin and laminin, orchestrated successful migration, adhesion and maturation of re-populated of rat hepatocytes. The preserved structural and biochemical ECM components aided in ameliorating the biological function of the hepatocytes leading to significant albumin and urea production in the culture medium.

The gene expression of the liver specific cell types in the recellularized rat liver matrix also confirms the integration of the parenchymal cells. The 2-3-fold increase in expression of albumin, CK-19 genes confirms the presence of required liver tissue microenvironment and vasculature for organ regeneration. The hepatocytes survival within the liver scaffold may be attributed to the vital cell-ECM interactions and structural stimuli directing their growth and differentiation. Balestrini et al. also demonstrated that there is divergent matrix conservation with respect to species it is likely that species-dependent native cues inherent to liver ECM may have profound effects on the suitability of the rat hepatocytes [30]. The repopulated cells are known to essentially transform native ECM to reinstate functional properties of regenerated organs by initialing the integration of native scaffold protein components [31]. Production of bioengineered livers for transplantation in patients with chronic liver failure would have an enormous impact to overcome the problem of donor organ shortage. Advancement in the identification of readily expandable cell type for repopulation is required to develop an appropriate functional tissue with minimal risk on transplantation [32].

## Conclusion

In conclusion, successfully recellularized liver scaffolds can be further aimed in designing natural 3D tissue constructs towards the fabrication of functional tissue and organ. We summarized a preface for re-seeded acellular natural scaffold with a scope for development of efficient functional organ with its current research trajectory. However, further studies are required to determine the capability of the recellularized scaffolds as models for drug metabolism and *in vivo* whole organ regeneration.

## Acknowledgements

We acknowledge Department of Science and Technology (DST), SERB (Science and Engineering Research Board), Government of India for providing grant to Dr. Tanya Debnath under National Post-Doctoral Fellow Scheme (N-PDF), Grant no. PDF/2016/003465. We also thank Dr. Meenakshi P and Bala Kishan for their efforts and help.

## Declaration of Potential Conflict of Interest

The authors declare that there is no conflict of interest.

## References

1. Gilbert TW (2012) Strategies for tissue and organ decellularization. *J Cell Biochem* 113: 2217-2222.
2. Debnath T, Shalini U, Kona LK, Vidya SJVS, Kamaraju SR, et al. (2015) Development of 3D alginate encapsulation for better chondrogenic differentiation potential than the 2D pellet system. *J Stem Cell Res Ther* 5: 276.
3. Tanya D, Sutapa G, Usha SP, Lakshmi K, Suguna RK, et al. (2015) Proliferation and Differentiation Potential of Human Adipose-Derived Stem Cells Grown on Chitosan Hydrogel. *PLoS ONE* 10: e0120803.
4. Hoshiba T, Lu H, Kawazoe N, Chen G (2010) Decellularized matrices for tissue engineering. *Expert Opin Biol Ther* 10: 1717-1728.
5. Ott HC, Matthies TS, Goh SK, Black LD, Kren SM (2008) Perfusion-decellularized matrix: using nature's platform to engineer a bioartificial heart. *Nat Med* 14: 213-221.
6. Petersen TH, Calle EA, Zhao L, Lee EJ, Gui L, et al. (2010) Tissue-engineered lungs for in vivo implantation. *Science* 329: 538-541.
7. Pei M, Li JT, Shoukry M, Zhang Y (2011) A review of decellularized stem cell matrix: A novel cell expansion system for cartilage tissue engineering. *Eur Cell Mater* 22: 333-343.
8. Sourav SP, Bo W, Benjamin W, Jason AW, Jun L (2014) Decellularized Scaffolds: Concepts, Methodologies, and Applications in Cardiac Tissue Engineering and Whole-Organ Regeneration. Chapter 3. *Tissue Regeneration: Where Nanostructure Meets Biology*. World Scientific Company Publisher.
9. Fung YC (1981) *Biomechanics: Mechanical Properties of Living Tissues*. 2nd edn. Springer-Verlag, New York, USA.
10. Chelluri LK (2012) *Stem cells and extracellular matrices*. Morgan & Claypool Publishers, Science.
11. Yuya M, Kentaro Y, Ken F, Takamichi I, Satoshi O, et al. (2017) A novel three-dimensional culture system maintaining the physiological extracellular matrix of fibrotic model livers accelerates progression of hepatocellular carcinoma cells. *Sci Rep* 7: 9827.
12. Lotze MT (2007) Damage-associated molecular pattern molecules. *Clin Immunol* 124: 1-4.
13. Badylak SF, Taylor D, Uygun K (2011) Whole-organ tissue engineering: decellularization and recellularization of three-dimensional matrix scaffolds. *Ann Rev Biomed Eng* 13: 27-53.
14. Denver MF, Justin DW, Stephen FB (2014) Decellularization and Cell Seeding of Whole Liver Biologic Scaffolds Composed of Extracellular Matrix. *J Clin Exp Hepatol* 5: 69-80.
15. Severgnini M, Sherman J, Sehgal A, Jayaprakash NK, Aubin J, et al. (2012) A rapid two-step method for isolation of functional primary mouse hepatocytes: cell characterization and asialoglycoprotein receptor-based assay development. *Cytotechnology* 64: 187-195.

16. Kmiec Z (2001) Cooperation of liver cells in health and disease. *Adv Anat Embryol Cell Biol* 161: 1-151.
17. Uygun BE, Soto-Gutierrez A, Yagi H, Izamis ML, Guzzardi MA, et al. (2010) Organ reengineering through development of a transplantable recellularized liver graft using decellularized liver matrix. *Nat Med* 16: 814-820.
18. Hussein KH, Park KM, Kang KS, Woo HM (2016) Biocompatibility evaluation of tissue engineered decellularized scaffolds for biomedical application. *Mater Sci Eng C* 67: 766-778.
19. Ming XP, Peng YH, Yuan C, Li QC, Xiao HR, et al. (2014) An efficient method for decellularization of the rat liver. *Journal of the Formosan Medical Association* 113: e680-e687.
20. Bo X, Joakim H, Vijay KK, Erik E, Suchitra SH (2016) Assessing rat liver-derived biomatrix for hepatic tissue engineering with human fetal liver stem cells. *Adv Tissue Eng Regen Med Open Access* 1: 00012.
21. Baldwin HS (1996) Early embryonic vascular development. *Cardiovasc Res* 31: e34-e45.
22. Wang X, Lin P, Yao Q, Chen C (2007) Development of small-diameter vascular grafts. *World J Surg* 31: 682-689.
23. Yeung BKS, Chong PYC, Petillo PA (2001) *Glycochemistry Principles, Synthesis and Applications*. In: Wang PG, Bertozzi CR (eds.). Marcel Dekker, New York City, NY, USA, p: 425.
24. Shyam SB, Sharon G, Rohit J, Martin LY (2016) Isolation and co-culture of rat parenchymal and non-parenchymal liver cells to evaluate cellular interactions and response. *Scientific Reports* 6: 25329.
25. Rui G, Wan-Quan W, Jun-Xi X, Yi L, Xinglong Z, et al. (2015) Hepatocyte culture in autologous decellularized spleen matrix. *Organogenesis* 11: 16-29.
26. Baptista PM, Siddiqui MM, Lozier G, Rodriguez SR, Atala A, et al. (2011) The use of whole organ decellularization for the generation of a vascularized liver organoid. *Hepatology* 53: 604-617.
27. Navarro-Tableros V, Herrera Sanchez MB, Figliolini F, Romagnoli R, Tetta C, et al. (2015) Recellularization of rat liver scaffolds by human liver stem cells. *Tissue Eng Part A* 21: 1929-1939.
28. Basak EU, Alejandro SG, Hiroshi Y, Maria-Louisa I, Maria AG, et al. (2010) Organ reengineering through development of a transplantable recellularized liver graft using decellularized liver matrix. *Nat Med* 16: 814-820.
29. Fox IJ, Chowdhury JR, Kaufman SS, Goertzen TC, Chowdhury NR, et al. (1998) Treatment of the Crigler-Najjar syndrome type I with hepatocyte transplantation. *N Engl J Med* 338: 1422-1426.
30. Balestrini JL, Gard AL, Gerhold KA, Wilcox EC, Liu A, et al. (2016) Comparative biology of decellularized lung matrix: Implications of species mismatch in regenerative medicine. *Biomaterials* 102: 220-230.
31. Yunfan H, Feng L (2016) Development of synthetic and natural materials for tissue engineering applications using adipose stem cells. *Stem Cells Int* 2016: 5786257.
32. Yesmin S, Paget MB, Murray HE, Downing R (2017) Bio-scaffolds in organ-regeneration: Clinical potential and current challenges. *Current Research in Translational Medicine* 65: 103-113.